iScience

CellPress
OPEN ACCESS

Article

Proteomic analysis identifies PFKP lactylation in SW480 colon cancer cells

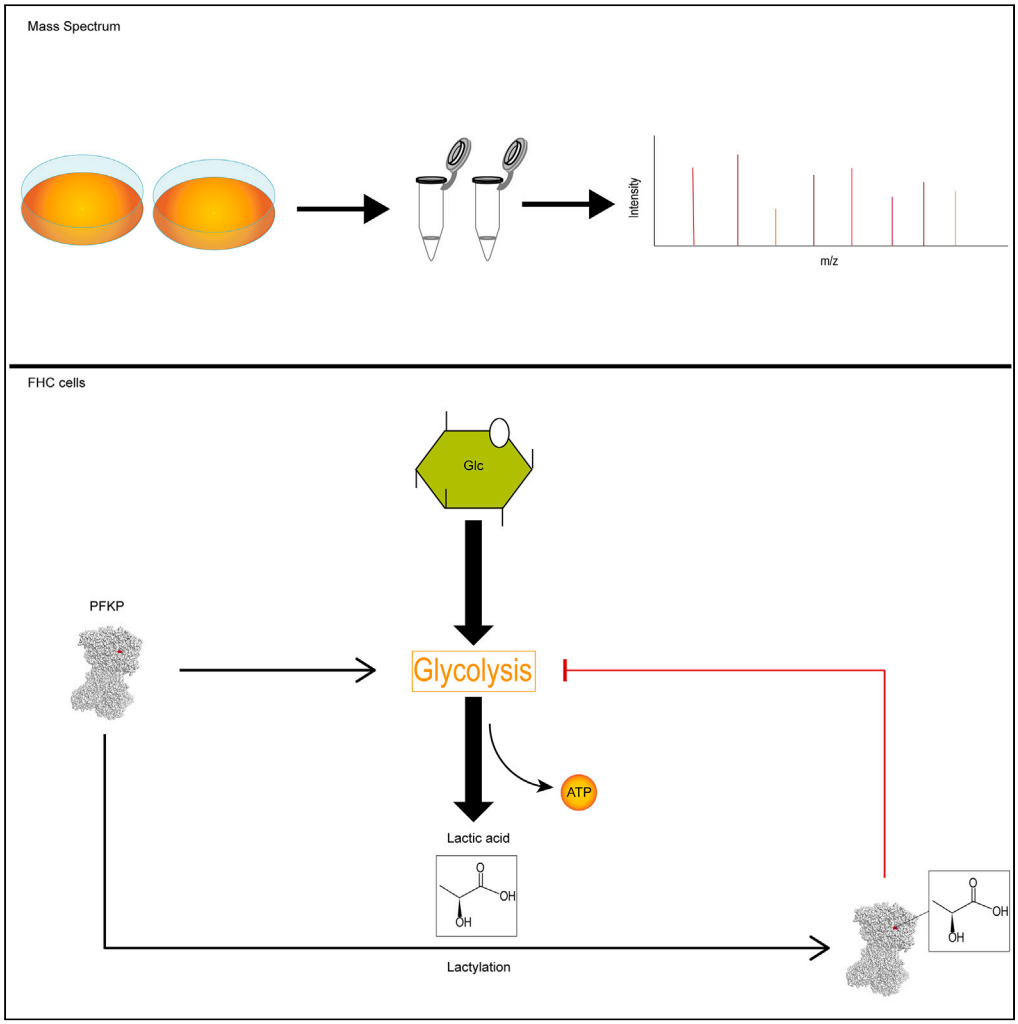

Zhe Cheng, Huichao Huang, Maoyu Li, Yongheng Chen

maoyuli@126.com (M.L.)
yonghenc@163.com (Y.C.)

Highlights

Protein lactylation in FHC and SW480 cells is identified through mass spectrometry

Lactylated proteins are significantly enriched in glycolysis pathway

PFKP lactylation is validated in CRC cells and tissues

Lactylation of PFKP attenuates its enzyme activity

Cheng et al., iScience 27, 108645
January 19, 2024
https://doi.org/10.1016/j.isci.2023.108645

iScience

CellPress
OPEN ACCESS

Article

Proteomic analysis identifies PFKP lactylation in SW480 colon cancer cells

Zhe Cheng,[1,4] Huichao Huang,[2,4] Maoyu Li,[3,*] and Yongheng Chen[3,5,*]

SUMMARY

Aerobic glycolysis is a pivotal hallmark of cancers, including colorectal cancer. Evidence shows glycolytic enzymes are regulated by post-translational modifications (PTMs), thereby affecting the Warburg effect and reprograming cancer metabolism. Lysine lactylation is a PTM reported in 2019 in histones. In this study, we identified protein lactylation in FHC cells and SW480 colon cancer cells through mass spectrometry. Totally, 637 lysine lactylation sites in 444 proteins were identified in FHC and SW480 cells. Lactylated proteins were enriched in the glycolysis pathway, and we identified lactylation sites in phosphofructokinase, platelet (PFKP) lysine 688 and aldolase A (ALDOA) lysine 147. We also showed that PFKP lactylation directly attenuated enzyme activity. Collectively, our study presented a resource to investigate proteome-wide lactylation in SW480 cells and found PFKP lactylation led to activity inhibition, indicating that lactic acid and lactylated PFKP may form a negative feedback pathway in glycolysis and lactic acid production.

INTRODUCTION

Colorectal cancer (CRC) is the third leading cause of cancer-related mortality worldwide, accounting for over 1.85 million cases and 850 thousand fatalities per year.[1,2] Due to the poor prognosis and the high risk of metastasis, CRC remains a significant problem for the community.[3] Consequently, it is necessary to investigate the mechanisms underlying the initiation and progression of CRC, which will accelerate the quest for novel diagnostic biomarkers and the development of an effective therapeutic target.

Reprogramming of energy metabolism, including aerobic glycolysis, aberrant lipid metabolism, amino acid metabolism, and mitochondrial biogenesis,[4] is a defining characteristic of cancer. Aerobic glycolysis, also known as the "Warburg effect", is the most characterized type of glycolysis, which means that, even in the presence of oxygen, cancer cells metabolize pyruvate into lactic acid instead of transporting pyruvate into the mitochondria for oxidative phosphorylation. This metabolic reprogramming is favored by cancers to sustain the rapid growth and proliferation demands of tumor cells.[5,6] Lactic acid, which was previously believed to be a byproduct of glycolysis, has been shown to play a critical role in regulating a number of biological processes, including tumor initiation and progression, macrophage polarization, and T helper cell differentiation.[7,8]

Post-translational modifications (PTMs) of proteins, such as protein phosphorylation and acylation, perform essential roles in cellular metabolism, signal transduction and tumorigenesis. Moreover, it can regulate the conformation, stability and functions of protein.[9–11] In recent years, numerous cellular metabolites have been discovered to be involved in protein acylation. The acylation forms include propionylation, butyrylation, and succinylation.[12] These protein acylations necessitate a particular modification substrate source. For instance, acetyl-CoA, which is derived from citrate by ATP citrate lyase (ACL),[13] is the major source of acetylation. The short chain fatty acids (SCFA) cognate to the lysine propionylation, butyrylation and succinylation metabolites can provide the precursors[14] and acyl-CoA synthetase 2 (ACSS2) catalyzes this transition. Propionyl-CoA is also derived from the catabolism of amino acid.[15] These non-metabolic functions provide valuable hints for the development of more efficient anti-cancer therapies. Recent research has demonstrated that lactic acid-derived histone lysine lactylation is a novel PTM.[16] Histone lactylation regulates gene expression, macrophage polarization, somatic cell reprogramming, and tumorigenesis.[17–19] Several studies on hepatocellular and gastric cancers have been conducted on non-histone proteins. These studies demonstrated that lysine lactylation is prevalent in a variety of malignancies and that the lactylation levels of specific proteins correlate with the prognosis of the patient.[20,21] These studies increase our understanding of the cancer specific lactylome. However, the global lactylome in certain CRC cells and tissues have not been reported.

[1]Department of Oncology, NHC Key Laboratory of Cancer Proteomics, Laboratory of Structural Biology, Xiangya Hospital, Central South University, Changsha, Hunan 410008, China
[2]Department of Infectious Disease, NHC Key Laboratory of Cancer Proteomics, Laboratory of Structural Biology, Xiangya Hospital, Central South University, Changsha, Hunan 410008, China
[3]Department of Oncology, NHC Key Laboratory of Cancer Proteomics, Laboratory of Structural Biology, National Clinical Research Center for Geriatric Disorders, Xiangya Hospital, Central South University, Changsha, Hunan 410008, China
[4]These authors contributed equally
[5]Lead contact
*Correspondence: maoyuli@126.com (M.L.), yonghenc@163.com (Y.C.)
https://doi.org/10.1016/j.isci.2023.108645

In this study, we identified and quantified the lysine lactylome in SW480 colon cancer cells. In total, 637 lactylation sites on 444 lactylated proteins, including histone and non-histone proteins, were identified. The characteristics and functions of lactylated proteins were uncovered by performing in-depth bioinformatics analyses. Lactylation of non-histone proteins is highly enriched in glycolysis processes, such as aldolase A (ALDOA) and phosphofructokinase, platelet (PFKP). In addition, immunoprecipitation (IP) and two-dimensional gel electrophoresis were used to confirm the lactylation of histone and non-histone proteins. Moreover, we investigated the role of lactylated PFKP in glycolysis in FHC cells and found that glycolysis-PFKP lactylation may constitute a negative feedback pathway in FHC cells. Overall, the study's findings provide a valuable resource for research into the specific functional roles of lactylation in SW480 CRC cells.

RESULTS

Systematic profiling of lysine lactylation proteome in SW480 cells

Reprogramming of energy metabolism is one of the hallmarks of tumor, with aerobic glycolysis being the most extensively researched. Thus, cancer cells preferentially convert pyruvate into lactic acid, the final product of glycolysis, even in the presence of oxygen.[22] As illustrated in Figure 1A, we initially evaluated pan-lysine lactylation (pan-Kla) using a Western blot assay. Different pan-Kla signals were detected in SW480 and FHC, suggesting that protein lactylation may vary in the two colon cells.

To systematically investigate the lactylation pattern in CRC, we performed quantitative lactylated proteomics of FHC and SW480 cells by affinity-based mass spectrometry. Figure 1B depicts the workflow of the lactylated proteomics analysis. Briefly, proteins were extracted from cells and digested with trypsin, and then the lactylated peptides were enriched with anti-Pan Kla antibody. Peptides were identified by liquid chromatography/tandem mass spectroscopy (LC-MS/MS) analysis and database searching. In total, 1,722 peptides were identified in 35,834 spectrums, and 637 lactylation sites in 444 lactylated proteins were quantified (Figure 1C). Among these lactylated proteins, 412 proteins had 1 lactylated sites or 2 lactylated sites, while a minor number had more lactylated sites (Figure 1D). Lactylated site of ALDOA K147 was shown in Figure 1E.

Functional characteristic analysis of lysine lactylation proteins

To gain a comprehensive understanding of the cellular functions of differentially lactylated proteins, we conducted an extensive bioinformatics analysis, including KOG (Eukaryotic Orthologous Group) and KEGG (Kyoto Encyclopedia of Genes and Genomes) pathway analyses, to uncover protein domain characteristics. We analyzed the protein categories, functions, and localizations of lactylated proteins to identify the amino acid sequences surrounding the Kla sites and validate potential Kla motifs. Two conserved motifs were identified: IxK (32 peptides) and KxxxxF (17 peptides) (Figure 2A). KOG analysis was performed, revealing the top ten pathways enriched with lactylated proteins (Figure 2B). Notably, lactylated proteins were found to be significantly enriched in pathways related to carbohydrate transport and metabolism, indicating a potential impact of Kla on cellular energy metabolism. To further characterize lactylated proteins in FHC and SW480 cells, we analyzed their subcellular localizations. The results showed that 47.95% of lactylated proteins were located in the nucleus, 15.31% in the cytoplasm, and 11.08% in the chromosome (Figure 2C). Additionally, KEGG analysis confirmed the enrichment of lactylated proteins in key pathways such as glycolysis and gluconeogenesis, DNA replication, nucleotide excision repair, and spliceosome, which aligned with the findings from KOG results (Figure 2D). Taken together, these findings suggest that lactylated proteins in FHC and SW480 cells are involved in essential physiological processes, with a notable enrichment in glycolytic processes.

Lactylation marks were detected on histones

Initially, lactylation was identified on histone proteins and implicated in the regulation of gene transcription and DNA replication.[16,23] In this study, we have identified 22 lactylation sites on histones in FHC and SW480 cells. Figure 3A illustrates both the previously studied and newly discovered histone lactylation sites. Figure 3B displays the top 10 histone lactylation sites with varying lactylation levels in FHC and SW480 cell lines. Several of these sites, including H2A.V K120, H3K14la, H4K8la, H4K12la and H3K23la, have been previously reported to undergo lactylation.[24–26] Furthermore, we validated three lactylation marks H4K12la, H3K14la and H4K8la using commercially available antibodies (Figure 3C). Western blotting (WB) confirmed the lactylation levels of H3K14, H4K8, and H4K12 in FHC, SW480, SW620, and HCT116 cell lines (Figure 3D). Despite the existence of additional lactylation sites detected by LC-MS, their validation was hindered by the unavailability of specific antibodies (Figure 3A). These findings collectively demonstrate the ability of spectrometry data to uncover information regarding both histone lactylation and non-histone lactylation.

Wide lactylation revealed on glycolytic enzymes

Based on our bioinformatic analysis, we observed that lactylated proteins predominantly localized in the cytoplasm, particularly those involved in glycolysis, such as PFKP, ALDOA, GAPDH, and ENO1 (Table S1, all lactylated proteins identified by mass spectrometry). In Figure 4A, these enzymes are highlighted in red, alongside the depiction of the glycolysis process and its associated reactants. Notably, PFKP and ALDOA play crucial roles within the glycolysis pathway.

ALDOA is responsible for the reversible conversion of fructose-1,6-bisphosphate into glyceraldehyde 3-phosphate and dihydroxyacetone phosphate. Mass spectrometry results demonstrated a significantly higher lactylation level of ALDOA in FHC cells compared to SW480 cells (Figure 4B). Subsequently, we experimentally evaluated the lactylation of ALDOA in multiple CRC cell lines using IP and WB. The lactylation of ALDOA was confirmed in FHC and HCT116 cell lines but not in SW480 and SW620 cell lines (Figure 4C). Two-dimensional gel electrophoresis

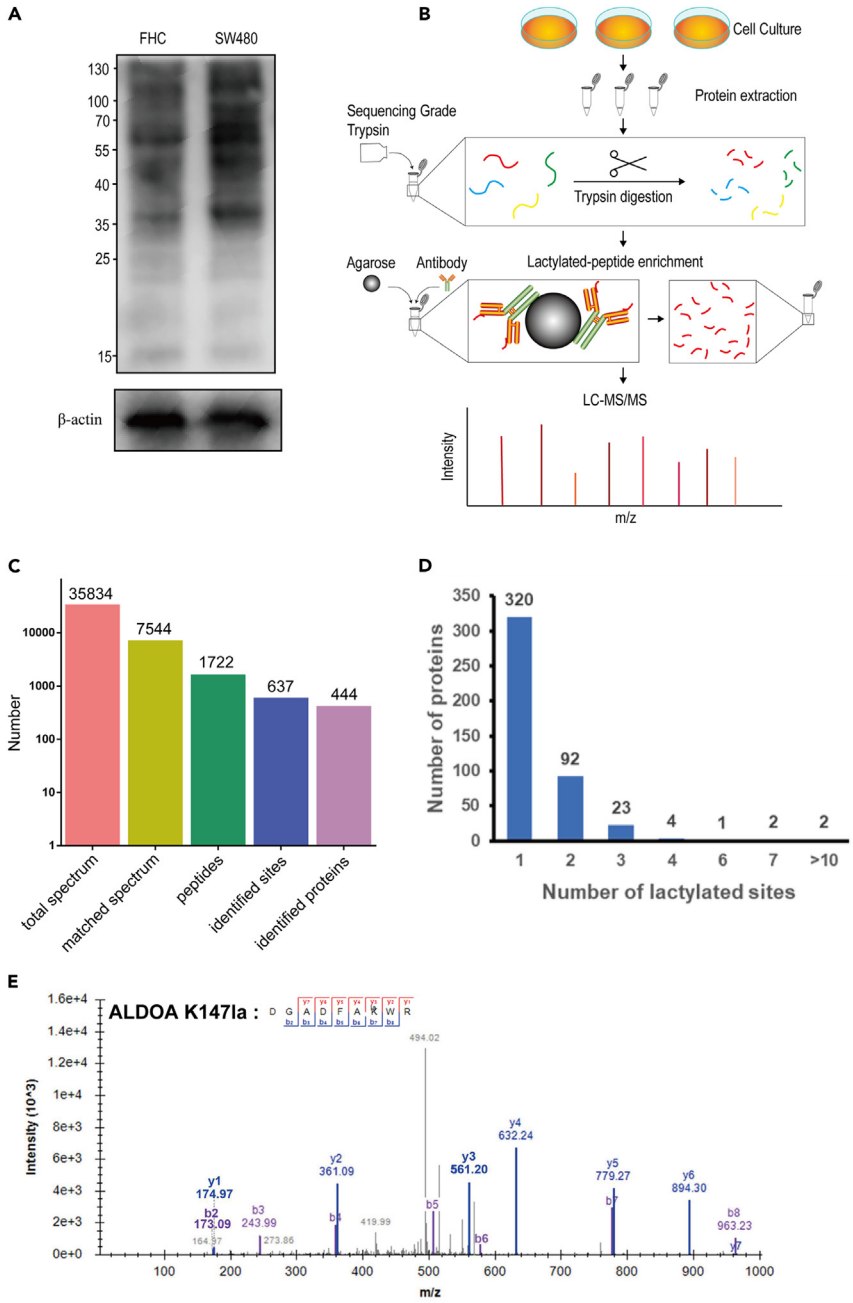

Figure 1. Systematic profiling of lysine lactylation proteome in SW480 cells

(A) Lactylated proteins in FHC and SW480 cells detected by anti-Pan Kla antibody.

(B) Workflow of the lactylated proteomics analysis in FHC and SW480 cell lines. The proteins were extracted from colon cells and digested with sequencing grade trypsin. Then the lactylated peptides were enriched by agarose-based immunoreaction. The lactylated peptides were analyzed by mass spectrometry using label-free quantification method to map the lactylome in SW480 cells.

(C) Number of peptides, peptides with identified lactylated sites and identified proteins detected by mass spectrometry.

(D) Number of proteins with different number of lactylated sites detected by mass spectrometry.

(E) Lactylated site of ALDOA K147la identified by mass spectrometry.

(2-DE) further validated this pattern, as the ALDOA signal in FHC cells exhibited a negative shift in comparison to that in SW480 cells (Figure 4D). It has been previously reported that lactylation of ALDOA at K147 can decrease its enzyme activity.[27] Consequently, these findings indicate the lactylation of the non-histone protein ALDOA and suggest a potential reduction in enzyme activity due to lactylation.

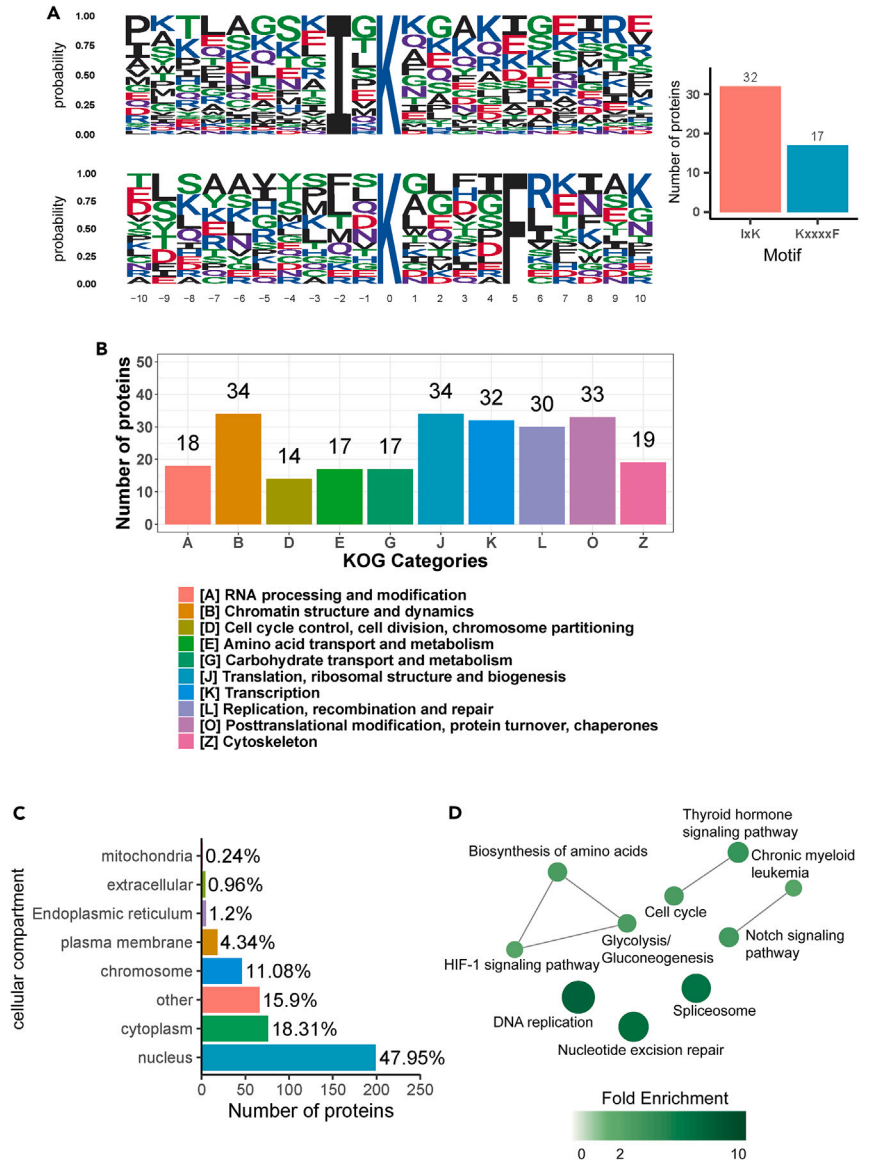

Figure 2. Properties of lactylated peptides in CRC

(A) Sequence motif logo showing a representative sequence for all Kla sites. The central K represents the lactylated lysine. Representative sequence for Kla sites showed by sequence motif logo. The central K represents the lactylated lysine. Two identified conserved motifs in the samples were shown below.

(B) KOG pathway analysis of lactylated proteins in FHC and SW480 cells.

(C) Subcellular localization analysis of lactylated proteins in FHC and SW480 cells.

(D) KEGG pathway analysis of lactylated proteomic results in FHC and SW480 cells.

PFKP is lactylated in SW480 cells and CRC tissues

PFKP represents the platelet isoform of phosphofructokinase (PFK) and plays a crucial role in glycolysis by catalyzing the irreversible conversion of fructose 6-phosphate to fructose 1,6-bisphosphate (Figure 4A). Figure 5A represents the representative spectrum of the lactylated mark at K688 on PFKP. Mass spectrometry results demonstrated a higher lactylation level of PFKP in FHC cells compared to SW480 cells (Figure 5B). To validate PFKP lactylation, WB and IP assays were performed. The results revealed PFKP lactylation in all tested cell lines, including FHC, SW480, SW620, and HCT116 (Figure 5C). Two-dimensional gel electrophoresis further confirmed this pattern, showing that PFKP signal migrated toward the positive side of the gel strip in SW480 cells compared to FHC cells, indicating a higher lactylation level in FHC cell lines (Figure 5D), consistent with the mass spectrometry findings. This phenomenon was further observed in four pairs of CRC tissues and matched adjacent normal tissues (Figures 5E and S1A), with clinical characteristics of the patients presented in Table S2. The patients showing reduced PFKP lactylation in cancer tissues ranked T2 and T4 in TNM staging. These results show that PFKP is not only lactylated in colon cells, but also in CRC

A

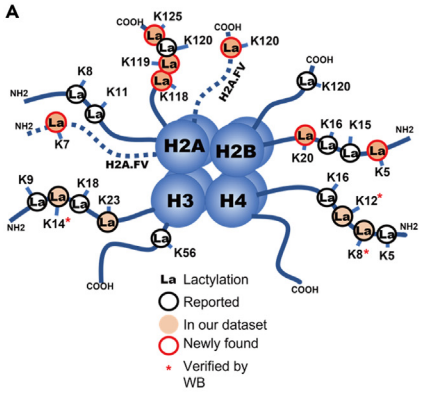

B

Histone	Lactylated site	Motif type
Reported		
H2A.V	K120	II
H3	K14	I
H4	K8	I
H4	K12	I
H3	K23	I
Newly found		
H2A	K118	I
H2A.V	K7	I
H2A	K119	II
H2B	K5	I
H2B	K20	I

C

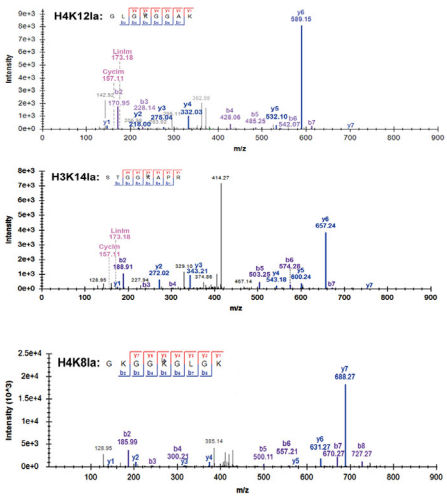

D

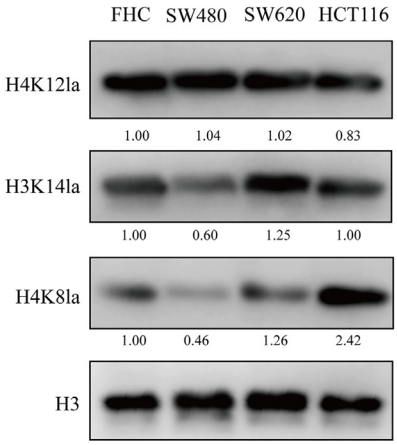

Figure 3. Lactylated histone proteins were detected by MS

(A) Schematic diagram of reported and newly found histone lactylation sites.

(B) Top 10 histone lactylated sites with different lactylation level in FHC and SW480 cell lines, previously reported and newly found sites included.

(C) Lactylated sites of H4K12, H3K14, and H4K8 identified by mass spectrometry.

(D) WB validation of H3K14, H4K8, and H4K12 lactylation in FHC, SW480, SW620, HCT116 cell lines.

paired tissues. However, statistical analysis of the association of PFKP lactylation and CRC prognosis is hindered by lack of PFKP site-specific lactylation antibody. To investigate the functional significance of PFKP lactylation in CRC, we performed crystal structure analysis of PFKP, highlighting the lactylated site in red (Figure 5F). Given that PFKP is a critical rate-limiting enzyme in glycolysis, the significant abundance of K688 lactylation raises the question of whether this modification affects its function. Considering the spatial proximity of K688 to the substrate binding site of PFKP, we hypothesize that lactylation at K688 may disrupt its enzyme activity, thus impacting the glycolysis pathway.

PFKP lactylation directly attenuates enzyme activity

The aforementioned findings indicate that the level of lactic acid regulates the lactylation of PFKP (la-PFKP), thereby modulating its activity in glycolysis in FHC cells. This discovery led us to speculate that changes in PFKP activity caused by PFKP lactylation forms a negative feedback loop in FHC cells. To validate this hypothesis, we first employed sodium dichloroacetate (DCA) and rotenone to manipulate lactic acid production by modulating the activities of pyruvate dehydrogenase (PDH) and mitochondrial respiratory chain complex I, respectively. As expected, intracellular lactic acid levels were significantly reduced upon DCA treatment but dramatically increased following rotenone induction (Figure 6A). Subsequently, we evaluated the corresponding lactylation levels upon DCA and rotenone treatments. WB analysis demonstrated a robust reduction in protein lactylation levels after DCA treatment, while a remarkable enhancement was observed upon rotenone induction (Figure 6B). Furthermore, two-dimensional gel electrophoresis revealed a potentiated lactylation pattern in FHC cells. Specifically, PFKP migrated toward the positive side of the gel strip following DCA treatment, whereas it shifted toward the negative side in the control and rotenone treatment groups (Figure 6C). We

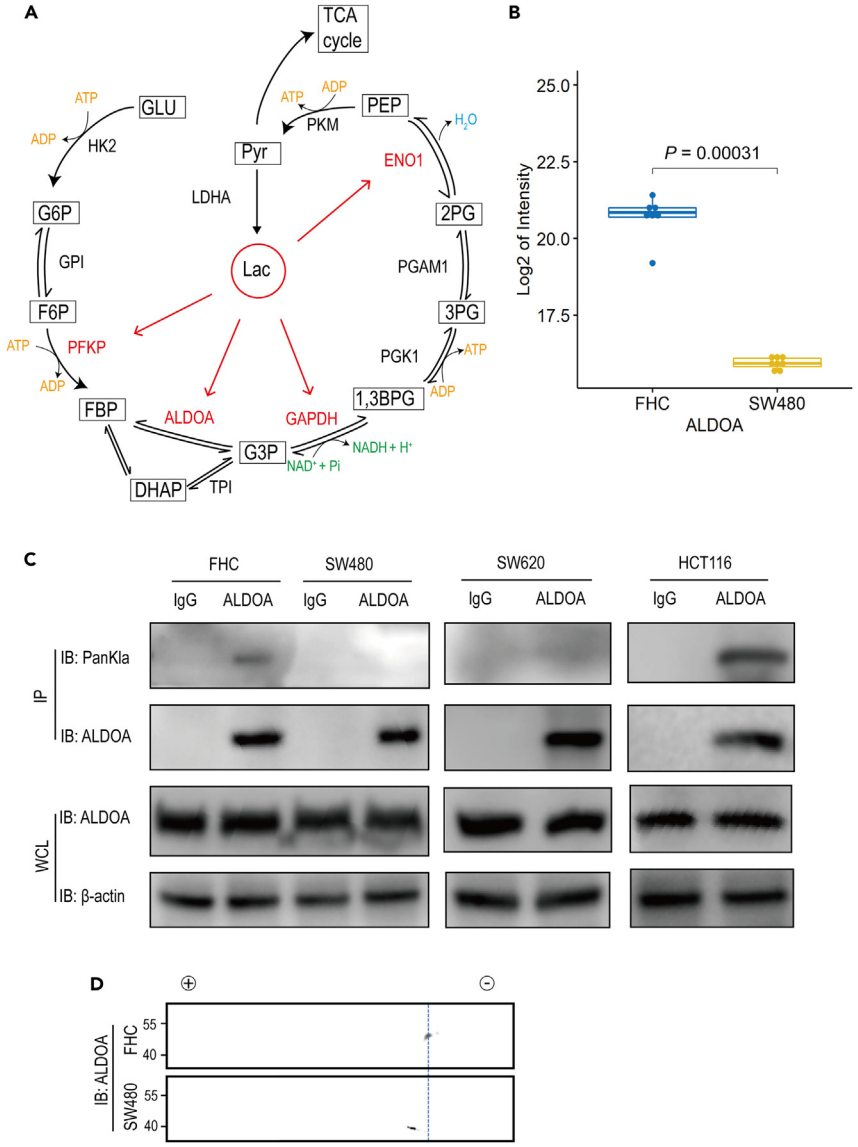

Figure 4. Wide lactylation revealed on glycolytic enzymes

(A) A comprehensive diagram form of glycolysis process. Lactylated enzymes PFKP, ALDOA, GAPDH, and ENO1 were labeled in red. Abbreviations: GLU, glucose; HK2, hexokinase 2; G6P, glucose 6-phosphate; GPI, glucose-6-phosphate isomerase; F6P, fructose-6-phosphate; FBP, fructose 1,6-bisphosphate; G3P, glycerol-3-phosphate; DHAP, dihydroxyacetone phosphate; TPI, triose-phosphate isomerase; GAPDH, lyceraldehyde 3-phosphate dehydrogenase; NAD+, nicotinamide adenine dinucleotide; 1,3BPG, 1,3-bisphosphoglyceric acid; PGK1, phosphoglycerate kinase 1; 3PG, 3-phosphoglyceric acid; PGAM1, phosphoglycerate mutase 1; 2PG, 2-phosphoglyceric acid; ENO1, enolase 1; PEP, phosphoenol pyruvate; PKM, pyruvate kinase isozymes M1/M2; Pyr, pyruvate; LDHA, lactate dehydrogenase A; Lac, lactic acid; ATP: adenosine 5′-triphosphate; ADP, adenosine diphosphate.

(B) ALDOA lactylation level is significantly higher in FHC cells than in SW480 cells based on MS data. Data represented with the mean ± SEM. (n = 3 biological replicates per group) and the p value was calculated with Wilcoxon rank-sum test.

(C) IP validation of ALDOA lactylation in FHC, SW480, SW620, and HCT116 cell lines. Lactylated ALDOA was detected by anti-Pan Kla antibody in FHC and HCT116 cell lines. Lactylated ALDOA was not detected in SW480 and SW620 cell lines.

(D) 2-DE of ALDOA in FHC and SW480 cell lines. ALDOA signal in FHC cells, shifted to the negative pole of the gel strip in comparison to that in SW480 cells.

further conducted the PFKP IP. The result showed that PFKP lactylation was reduced upon DCA treatment and was elevated upon rotenone treatment (Figure S1B). These observations suggest that inhibiting endogenous lactic acid production decreases PFKP lactylation in FHC cells.

To determine whether PFKP activity is regulated by endogenous lactic acid levels, we tested PFKP enzyme activity following DCA and rotenone treatments. The analysis revealed that PFKP activity was significantly enhanced with reduced PFKP lactylation upon DCA treatment, whereas it was attenuated with increased PFKP lactylation upon rotenone treatment (Figure 6D). Collectively, these results support the notion

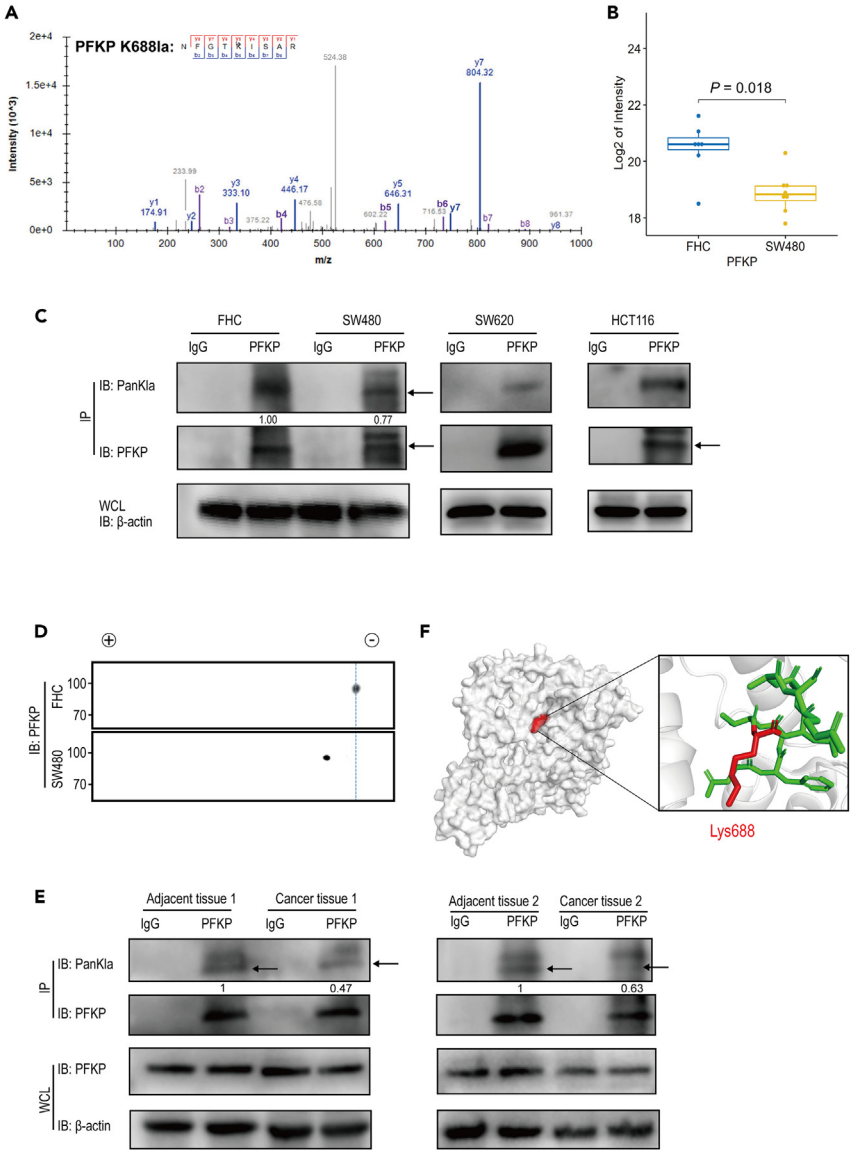

Figure 5. Validation of PFKP lactylation in CRC cells and tissues

(A) Representative spectrum of PFKP K688la mark.

(B) PFKP lactylation level is statistically higher in FHC cells than in SW480 cells based on MS data. Data represented with the mean ± SEM. (n = 3 biological replicates per group) and the p value was calculated with Wilcoxon rank-sum test.

(C) IP validation of PFKP lactylation in FHC, SW480, SW620, and HCT116 cell lines. Lactylated PFKP was detected by anti-Pan Kla antibody in all cell lines. The arrows indicate the PFKP bands detected by the PFKP antibody.

(D) 2-DE of PFKP in FHC and SW480 cell lines. PFKP signal in SW480 cells migrated to the positive side of the gel strip in comparison to that in FHC cells.

(E) IP validation of PFKP lactylation in CRC tissue. Lactylated PFKP was detected both in adjacent tissue and cancer tissue and PFKP lactylation level was downregulated in the cancer tissue. The arrows indicate the PFKP bands detected by the PFKP antibody.

(F) Crystal structure of human PFKP (PDB: 4WL0) with newly identified lactylation site K688la highlighted in red.

that PFKP activity is dramatically suppressed by PFKP lactylation, thereby establishing a negative feedback mechanism in FHC cells. This implies that when the glycolysis pathway is overactivated and excessive lactic acid is produced, the activity of the upstream enzyme PFKP is inhibited through lactylation, leading to a dampened glycolytic flux and decreased lactic acid levels.

DISCUSSION

Most cancer cells primarily rely on aerobic glycolysis to support rapid growth, proliferation, and biosynthesis of biomolecules, such as nucleotides, amino acids and lipids.[28,29] Aerobic glycolysis, a key metabolic feature of tumors, significantly affects gene expression, cellular

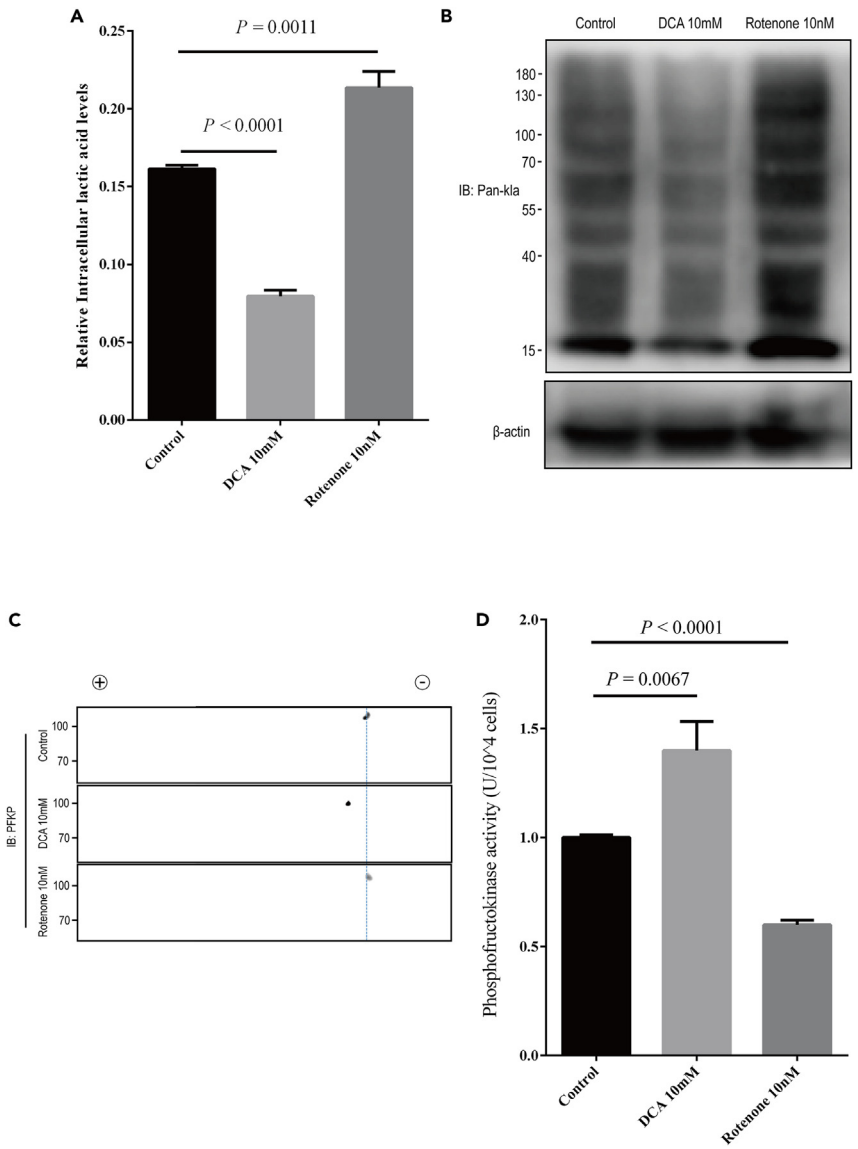

Figure 6. PFKP lactylation directly attenuates enzyme activity

(A) Intracellular lactate level of FHC cells in control, 10 mM DCA and 10 nM Rotenone group. Data represent the mean ± SEM. (n = 3 biological replicates per group) and the p value was calculated by an unpaired two-tailed Student's *t* test.

(B) WB result presenting protein lactylation level in control, 10 mM DCA and 10 nM Rotenone group.

(C) 2-DE test of PFKP lactylation level in control, 10 mM DCA and 10 nM Rotenone group.

(D) PFKP activity in control, 10 mM DCA and 10 nM Rotenone group. Data represent the mean ± SEM. (n = 3 biological replicates per group) and the p value was calculated by an unpaired two-tailed Student's *t* test.

differentiation, and the tumor microenvironment (TME).[30,31] Glycolysis is regulated by various factors, including oncogenes, tumor suppressors, non-coding RNAs, and metabolites.[32–34] Lactic acid, previously considered a byproduct of glycolysis, has been found to play a crucial role in modulating diverse biological processes, including tumor initiation and progression, macrophage polarization, and T helper cell differentiation.[35,36] In 2019, it was discovered that lactic acid can induce a novel modification of histone proteins known as histone lactylation.[16] In this study, we investigate the lactylation profile and characteristics in SW480 CRC cells. In addition to histone lactylation, we identify lactylation in non-histone proteins. We validate lysine lactylation in both histone and non-histone proteins. Furthermore, we uncover that a glycolysis/la-PFKP/lactic acid negative feedback loop may exist in FHC cells.

Lysine acylations, including lysine lactylation, have emerged as crucial protein modifications in CRC. Previous studies have explored global alterations of histone acetylation in CRC tissues.[37] And non-histone protein acetylation has been linked to CRC invasion and metastasis.[38,39] Lysine lactylation, a novel form of lysine acylation, has garnered significant interest in the fields of macrophage polarization, infectious diseases,

and tumorigenesis.[40] Both histone and non-histone protein lactylation have been implicated in various pathophysiological processes, including oncogenesis. However, a comprehensive analysis of global lysine lactylation in CRC cells and tissues has not been reported to date. In this study, we employed quantitative proteomics and a pan-lysine lactylation antibody to investigate the overall lactylated proteome in SW480 cells. A total of 637 lactylation sites in 444 proteins, spanning diverse cellular locations and biological functions, were identified. Among these, 22 lactylation sites in histone proteins were detected, including two novel histone lactylation sites (H3K12la and H4K8la) that were reported and validated by WB for the first time in CRC cells. Additionally, we identified 440 non-histone proteins with 615 lactylation sites. Our findings align with previous studies demonstrating the involvement of histone protein lactylation in disease development. For instance, Pan et al. revealed that lactylation of H4K12 activated the transcription of glycolytic genes in macroglia, contributing to the pathogenesis of Alzheimer's disease.[25] Moreover, lactylation of H3K18 has been reported to activate the transcription of the m6A binding protein YTHDF2, promoting the degradation of tumor suppressor genes, PER1 and TP53, thus elucidating a novel mechanism of histone lactylation in tumorigenesis.[19]

In our study, the lactylation profile in SW480 cells exhibits that lactylation proteins are enriched in glycolysis, biosynthesis of amino acids, DNA replication, nucleotide excision repair and spliceosome. Similar results were observed in AGS gastric cancer cells (a human gastric adenocarcinoma cell line).[21] In hepatocellular cancer (HCC) tissues lactylation proteins were enriched in glycolysis, ribosome and pentose phosphate pathway. However, proteins associated with fatty acid oxidation, glutamine metabolism, ATP metabolism were also lactylated in HCC tissues rather than SW480 cells.[20] This may be because the liver and colon have different biological functions. In addition to histone lactylation, non-histone protein lactylation has also been implicated in various biological processes. However, due to the limited availability of lactylation-specific antibodies, only a few studies have focused on non-histone protein lactylation. In the context of polymicrobial sepsis, lactic acid was found to induce lactylation and acetylation of HMGB1, promoting its release from macrophages.[41] However, the specific lactylation sites in HMGB1 were not identified in that study. Another group analyzed the lysine lactylome in gastric cancer cells and suggested a potential link between non-histone protein lactylation and tumor progression.[21] Similarly, proteome-wide analyses of lactylated sites have been conducted in *T. brucei* and the plant fungal pathogen *Botrytis cinerea*.[42,43] However, these studies did not include experimental validation of protein lactylation or investigation of underlying mechanisms.

In our study, in addition to presenting the comprehensive lactylated proteome, we identified lactylation sites in two glycolysis-associated enzymes, ALDOA and PFKP, in CRC. Specifically, ALDOA was found to be lactylated at K147, while PFKP exhibited lactylation at K688 (Figures 1E and 5A). To validate the lactylation of ALDOA and PFKP, we performed IP and two-dimensional gel electrophoresis. Our results, consistent with the lactylome data, confirmed the presence of lactylation signals in PFKP both *in vitro* and *in vivo*. While previous studies have reported lysine lactylation in ALDOA in various cell lines,[27] our work provides experimental evidence for lactylation in ALDOA and PFKP for the first time. Wan et al. incorporated an engineered lysine at the 147 residue that was attached with lactic acid subgroup to investigate the function of ALDOA lactylation. The result showed that the enzyme activity of lactylated ALDOA was reduced compared with wild-type ALDOA.[27] Besides, wide lactylation on glycolytic enzymes have also been observed in HCC.[20] Studies by Yang et al. investigated lysine lactylation in HCC tissues and adjacent tissues, revealing enrichment of lactylated proteins in glycolysis/gluconeogenesis pathways. They also demonstrated that lactylation of adenylate kinase 2 (AK2) at K28 contributes to energy disorder and HCC malignancy, although PFKP lactylation was not explored in their research. Our findings, on the other hand, add ALDOA and PFKP to the growing list of non-histone protein lactylation events and suggest new functions of these proteins in cancer development. It is highly likely that other non-histone proteins are lactylated in CRC, and further investigations will be necessary to identify and characterize these lactylation events and their roles in regulating diverse cellular processes, such as tumor initiation and progression.

It has been suggested that many glycolytic enzymes such as PKM2, ALDOA, PFK, and LDHA, are tightly modulated by diverse PTMs, thereby contribute to the Warburg effect and subsequently reprogram of cancer metabolism.[44–46] Recent studies have shown that c-Src phosphorylates HK1 (hexokinase 1) (Tyr732) and HK2 (Tyr686), the rate-limiting enzymes of glycolysis, promoting tumor proliferation and growth.[47] Zhao et al. demonstrated that lactylation of LDHA at K5 inhibits its activity, triggers lysosomal degradation through chaperone-mediated autophagy (CMA), and reduces cell proliferation and migration in pancreatic cancer.[48] Lee et al. previously reported that phosphorylation of PFKP at Y64 enhances PI3K/AKT-dependent PFK1 activation and GLUT1 (glucose transporter type 1) expression, promoting the Warburg effect, tumor cell proliferation, and brain tumorigenesis.[49] It has been recently discovered that PFKP overexpression accelerated CRC cell growth and motility by regulating cell cycle progression.[50] Guan et al. constructed a chronic stress mouse model and showed that chronic stress enhanced GLUT1, HK2, and PFKP expression, and promoted CRC progression in mice.[51] Our study revealed that reduced PFKP lactylation might increase the PFKP enzyme activity in both SW480 cells and human CRC tissues, which may promote the aerobic glycolysis and consequently contribute to CRC progression.

In our study, we observed that lactic acid-induced lactylation of PFKP suppresses its enzyme activity in FHC cells (Figure 6). We propose that FHC cells utilize a negative feedback mechanism involving lactylation-dependent inhibition of the rate-limiting enzyme PFKP in the glycolysis pathway (Figure S2), indicating the potential significance of dysregulated lactic acid/la-PFKP negative feedback loop in CRC initiation. However, how PFKP lactylation level is reduced upon DCA treatment and the mechanism that PFKP enzyme activity is regulated by its lactylation need further investigation. Meanwhile the specific lactylase responsible for lactylation of PFKP at K688 remains unidentified. Identification of such a lactylase would unveil crucial regulatory roles of PFKP lactylation in human cancer.

Limitations of the study

Our study has several limitations. Firstly, the mass spectrometry analysis was only performed on two cell lines. It would have been better if we could have performed lactylomic analysis in more cell lines. Secondly, it would have been better if we had performed lactylomic analysis on CRC tissue samples. Finally, the mechanism of PFKP lactylation in CRC needs to be further investigated.

STAR★METHODS

Detailed methods are provided in the online version of this paper and include the following:

- KEY RESOURCES TABLE
- RESOURCE AVAILABILITY
  - Lead contact
  - Materials availability
  - Data and code availability
- EXPERIMENTAL MODEL AND STUDY PARTICIPANT DETAILS
  - Clinical sample acquisition
  - Cell lines and cell culture
- METHOD DETAILS
  - Protein extraction and tryptic digestion
  - Lactylated-peptide enrichment
  - LC-MS/MS analysis
  - Peptide identification and protein quantification
  - Bioinformatic analysis
  - Histone extraction
  - Western blotting (WB)
  - Immunoprecipitation (IP)
  - Two-dimensional gel electrophoresis (2-DE)
  - Intracellular lactic acid determination and PFKP activity assay
- QUANTIFICATION AND STATISTICAL ANALYSIS

SUPPLEMENTAL INFORMATION

Supplemental information can be found online at https://doi.org/10.1016/j.isci.2023.108645.

ACKNOWLEDGMENTS

This work was financially supported by the Natural Science Foundation of China (No. 81974074 and 82172654); Hunan Provincial Science and Technology Department (2021RC4012 and 2022JJ40788); China Postdoctoral Science Foundation (2022M713512); the Youth Science Foundation of Xiangya Hospital (2022Q09); The Natural Science Foundation of Hunan Province (No.2021JJ31073).

AUTHOR CONTRIBUTIONS

Y.C. and M.L. conceived and supervised the project; Z.C. and H.H. performed the experiments; H.H. wrote the paper; Z.C. and H.H. revised the paper. All authors read and approved the final manuscript.

DECLARATION OF INTERESTS

The authors declare no competing interests.

Received: February 18, 2023
Revised: June 23, 2023
Accepted: December 1, 2023
Published: December 6, 2023

REFERENCES

1. Siegel, R.L., Miller, K.D., Goding Sauer, A., Fedewa, S.A., Butterly, L.F., Anderson, J.C., Cercek, A., Smith, R.A., and Jemal, A. (2020). Colorectal cancer statistics, 2020. CA. Cancer J. Clin. *70*, 145–164.
2. Biller, L.H., and Schrag, D. (2021). Diagnosis and Treatment of Metastatic Colorectal Cancer: A Review. JAMA *325*, 669–685.
3. Dekker, E., Tanis, P.J., Vleugels, J.L.A., Kasi, P.M., and Wallace, M.B. (2019). Colorectal cancer. Lancet *394*, 1467–1480.
4. Hanahan, D., and Weinberg, R.A. (2011). Hallmarks of cancer: the next generation. Cell *144*, 646–674.
5. Martínez-Reyes, I., and Chandel, N.S. (2021). Cancer metabolism: looking forward. Nat. Rev. Cancer *21*, 669–680.
6. Pavlova, N.N., and Thompson, C.B. (2016). The Emerging Hallmarks of Cancer Metabolism. Cell Metab. *23*, 27–47.
7. Li, Z., and Zhang, H. (2016). Reprogramming of glucose, fatty acid and amino acid metabolism for cancer progression. Cell. Mol. Life Sci. *73*, 377–392.
8. Certo, M., Tsai, C.H., Pucino, V., Ho, P.C., and Mauro, C. (2021). Lactate modulation of immune responses in inflammatory versus tumour microenvironments. Nat. Rev. Immunol. *21*, 151–161.
9. Blixt, O., Head, S., Mondala, T., Scanlan, C., Huflejt, M.E., Alvarez, R., Bryan, M.C., Fazio, F., Calarese, D., Stevens, J., et al. (2004). Printed covalent glycan array for ligand profiling of diverse glycan binding proteins. Proc. Natl. Acad. Sci. USA *101*, 17033–17038.
10. Krueger, K.E., and Srivastava, S. (2006). Posttranslational protein modifications: current implications for cancer detection,

prevention, and therapeutics. Mol. Cell. Proteomics *5*, 1799–1810.
11. Hoffman, M.D., Sniatynski, M.J., and Kast, J. (2008). Current approaches for global post-translational modification discovery and mass spectrometric analysis. Anal. Chim. Acta *627*, 50–61.
12. Sabari, B.R., Zhang, D., Allis, C.D., and Zhao, Y. (2017). Metabolic regulation of gene expression through histone acylations. Nat. Rev. Mol. Cell Biol. *18*, 90–101.
13. Wellen, K.E., Hatzivassiliou, G., Sachdeva, U.M., Bui, T.V., Cross, J.R., and Thompson, C.B. (2009). ATP-citrate lyase links cellular metabolism to histone acetylation. Science *324*, 1076–1080.
14. Xie, Z., Zhang, D., Chung, D., Tang, Z., Huang, H., Dai, L., Qi, S., Li, J., Colak, G., Chen, Y., et al. (2016). Metabolic Regulation of Gene Expression by Histone Lysine β-Hydroxybutyrylation. Mol. Cell *62*, 194–206.
15. Chen, Y., Sprung, R., Tang, Y., Ball, H., Sangras, B., Kim, S.C., Falck, J.R., Peng, J., Gu, W., and Zhao, Y. (2007). Lysine propionylation and butyrylation are novel post-translational modifications in histones. Mol. Cell. Proteomics *6*, 812–819.
16. Zhang, D., Tang, Z., Huang, H., Zhou, G., Cui, C., Weng, Y., Liu, W., Kim, S., Lee, S., Perez-Neut, M., et al. (2019). Metabolic regulation of gene expression by histone lactylation. Nature *574*, 575–580.
17. Irizarry-Caro, R.A., McDaniel, M.M., Overcast, G.R., Jain, V.G., Troutman, T.D., and Pasare, C. (2020). TLR signaling adapter BCAP regulates inflammatory to reparatory macrophage transition by promoting histone lactylation. Proc. Natl. Acad. Sci. USA *117*, 30628–30638.
18. Li, L., Chen, K., Wang, T., Wu, Y., Xing, G., Chen, M., Hao, Z., Zhang, C., Zhang, J., Ma, B., et al. (2020). Glis1 facilitates induction of pluripotency via an epigenome-metabolome-epigenome signalling cascade. Nat. Metab. *2*, 882–892.
19. Yu, J., Chai, P., Xie, M., Ge, S., Ruan, J., Fan, X., and Jia, R. (2021). Histone lactylation drives oncogenesis by facilitating m(6)A reader protein YTHDF2 expression in ocular melanoma. Genome Biol. *22*, 85.
20. Yang, Z., Yan, C., Ma, J., Peng, P., Ren, X., Cai, S., Shen, X., Wu, Y., Zhang, S., Wang, X., et al. (2023). Lactylome analysis suggests lactylation-dependent mechanisms of metabolic adaptation in hepatocellular carcinoma. Nat. Metab. *5*, 61–79.
21. Yang, D., Yin, J., Shan, L., Yi, X., Zhang, W., and Ding, Y. (2022). Identification of lysine-lactylated substrates in gastric cancer cells. iScience *25*, 104630.
22. Koppenol, W.H., Bounds, P.L., and Dang, C.V. (2011). Otto Warburg's contributions to current concepts of cancer metabolism. Nat. Rev. Cancer *11*, 325–337.
23. Hagihara, H., Shoji, H., Otabi, H., Toyoda, A., Katoh, K., Namihira, M., and Miyakawa, T. (2021). Protein lactylation induced by neural excitation. Cell Rep. *37*, 109820.
24. Yin, D., Jiang, N., Cheng, C., Sang, X., Feng, Y., Chen, R., and Chen, Q. (2022). Protein Lactylation and Metabolic Regulation of the Zoonotic Parasite Toxoplasma gondii. Genomics Proteomics Bioinformatics.
25. Pan, R.Y., He, L., Zhang, J., Liu, X., Liao, Y., Gao, J., Liao, Y., Yan, Y., Li, Q., Zhou, X., et al. (2022). Positive feedback regulation of microglial glucose metabolism by histone H4 lysine 12 lactylation in Alzheimer's disease. Cell Metab. *34*, 634–648.e6.
26. Yang, W., Wang, P., Cao, P., Wang, S., Yang, Y., Su, H., and Nashun, B. (2021). Hypoxic in vitro culture reduces histone lactylation and impairs pre-implantation embryonic development in mice. Epigenet. Chromatin *14*, 57.
27. Wan, N., Wang, N., Yu, S., Zhang, H., Tang, S., Wang, D., Lu, W., Li, H., Delafield, D.G., Kong, Y., et al. (2022). Cyclic immonium ion of lactyllysine reveals widespread lactylation in the human proteome. Nat. Methods *19*, 854–864.
28. Vander Heiden, M.G., Locasale, J.W., Swanson, K.D., Sharfi, H., Heffron, G.J., Amador-Noguez, D., Christofk, H.R., Wagner, G., Rabinowitz, J.D., Asara, J.M., and Cantley, L.C. (2010). Evidence for an alternative glycolytic pathway in rapidly proliferating cells. Science *329*, 1492–1499.
29. Vander Heiden, M.G., Cantley, L.C., and Thompson, C.B. (2009). Understanding the Warburg effect: the metabolic requirements of cell proliferation. Science *324*, 1029–1033.
30. Lunt, S.Y., and Vander Heiden, M.G. (2011). Aerobic glycolysis: meeting the metabolic requirements of cell proliferation. Annu. Rev. Cell Dev. Biol. *27*, 441–464.
31. Feng, J., Li, J., Wu, L., Yu, Q., Ji, J., Wu, J., Dai, W., and Guo, C. (2020). Emerging roles and the regulation of aerobic glycolysis in hepatocellular carcinoma. J. Exp. Clin. Cancer Res. *39*, 126.
32. Sun, L., Song, L., Wan, Q., Wu, G., Li, X., Wang, Y., Wang, J., Liu, Z., Zhong, X., He, X., et al. (2015). cMyc-mediated activation of serine biosynthesis pathway is critical for cancer progression under nutrient deprivation conditions. Cell Res. *25*, 429–444.
33. Bensaad, K., Tsuruta, A., Selak, M.A., Vidal, M.N.C., Nakano, K., Bartrons, R., Gottlieb, E., and Vousden, K.H. (2006). TIGAR, a p53-inducible regulator of glycolysis and apoptosis. Cell *126*, 107–120.
34. Hung, C.L., Wang, L.Y., Yu, Y.L., Chen, H.W., Srivastava, S., Petrovics, G., and Kung, H.J. (2014). A long noncoding RNA connects c-Myc to tumor metabolism. Proc. Natl. Acad. Sci. USA *111*, 18697–18702.
35. Brooks, G.A. (2020). Lactate as a fulcrum of metabolism. Redox Biol. *35*, 101454.
36. Sun, S., Li, H., Chen, J., and Qian, Q. (2017). Lactic Acid: No Longer an Inert and End-Product of Glycolysis. Physiology *32*, 453–463.
37. Karczmarski, J., Rubel, T., Paziewska, A., Mikula, M., Bujko, M., Kober, P., Dadlez, M., and Ostrowski, J. (2014). Histone H3 lysine 27 acetylation is altered in colon cancer. Clin. Proteomics *11*, 24.
38. Shen, Z., Wang, B., Luo, J., Jiang, K., Zhang, H., Mustonen, H., Puolakkainen, P., Zhu, J., Ye, Y., and Wang, S. (2016). Global-scale profiling of differential expressed lysine acetylated proteins in colorectal cancer tumors and paired liver metastases. J. Proteomics *142*, 24–32.
39. Jiang, H., Wu, L., Chen, J., Mishra, M., Chawsheen, H.A., Zhu, H., and Wei, Q. (2015). Sulfiredoxin Promotes Colorectal Cancer Cell Invasion and Metastasis through a Novel Mechanism of Enhancing EGFR Signaling. Mol. Cancer Res. *13*, 1554–1566.
40. Chen, A.N., Luo, Y., Yang, Y.H., Fu, J.T., Geng, X.M., Shi, J.P., and Yang, J. (2021). Lactylation, a Novel Metabolic Reprogramming Code: Current Status and Prospects. Front. Immunol. *12*, 688910.
41. Yang, K., Fan, M., Wang, X., Xu, J., Wang, Y., Tu, F., Gill, P.S., Ha, T., Liu, L., Williams, D.L., and Li, C. (2022). Lactate promotes macrophage HMGB1 lactylation, acetylation, and exosomal release in polymicrobial sepsis. Cell Death Differ. *29*, 133–146.
42. Gao, M., Zhang, N., and Liang, W. (2020). Systematic Analysis of Lysine Lactylation in the Plant Fungal Pathogen Botrytis cinerea. Front. Microbiol. *11*, 594743.
43. Zhang, N., Jiang, N., Yu, L., Guan, T., Sang, X., Feng, Y., Chen, R., and Chen, Q. (2021). Protein Lactylation Critically Regulates Energy Metabolism in the Protozoan Parasite Trypanosoma brucei. Front. Cell Dev. Biol. *9*, 719720.
44. Hitosugi, T., and Chen, J. (2014). Post-translational modifications and the Warburg effect. Oncogene *33*, 4279–4285.
45. Gao, X., Wang, H., Yang, J.J., Liu, X., and Liu, Z.R. (2012). Pyruvate kinase M2 regulates gene transcription by acting as a protein kinase. Mol. Cell *45*, 598–609.
46. Hitosugi, T., Fan, J., Chung, T.W., Lythgoe, K., Wang, X., Xie, J., Ge, Q., Gu, T.L., Polakiewicz, R.D., Roesel, J.L., et al. (2011). Tyrosine phosphorylation of mitochondrial pyruvate dehydrogenase kinase 1 is important for cancer metabolism. Mol. Cell *44*, 864–877.
47. Zhang, J., Wang, S., Jiang, B., Huang, L., Ji, Z., Li, X., Zhou, H., Han, A., Chen, A., Wu, Y., et al. (2017). c-Src phosphorylation and activation of hexokinase promotes tumorigenesis and metastasis. Nat. Commun. *8*, 13732.
48. Zhao, D., Zou, S.W., Liu, Y., Zhou, X., Mo, Y., Wang, P., Xu, Y.H., Dong, B., Xiong, Y., Lei, Q.Y., and Guan, K.L. (2013). Lysine-5 acetylation negatively regulates lactate dehydrogenase A and is decreased in pancreatic cancer. Cancer Cell *23*, 464–476.
49. Lee, J.H., Liu, R., Li, J., Wang, Y., Tan, L., Li, X.J., Qian, X., Zhang, C., Xia, Y., Xu, D., et al. (2018). EGFR-Phosphorylated Platelet Isoform of Phosphofructokinase 1 Promotes PI3K Activation. Mol. Cell *70*, 197–210.e7.
50. Lu, T.J., Yang, Y.F., Cheng, C.F., Tu, Y.T., Chen, Y.R., Lee, M.C., and Tsai, K.W. (2023). Phosphofructokinase Platelet Overexpression Accelerated Colorectal Cancer Cell Growth and Motility. J. Cancer *14*, 943–951.
51. Guan, Y., Yao, W., Yu, H., Feng, Y., Zhao, Y., Zhan, X., and Wang, Y. (2023). Chronic stress promotes colorectal cancer progression by enhancing glycolysis through β2-AR/CREB1 signal pathway. Int. J. Biol. Sci. *19*, 2006–2019.

STAR★METHODS

KEY RESOURCES TABLE

REAGENT or RESOURCE	SOURCE	IDENTIFIER
Antibodies		
Rabbit polyclonal anti-Pan Kla	PTM BIO	Cat# PTM-1401; RRID:AB_2868521
Rabbit polyclonal anti-H4K12la	PTM BIO	Cat# PTM-1411RM; RRID:AB_2941896
Rabbit polyclonal anti-H3K14la	PTM BIO	Cat# PTM-1414RM; RRID:AB_2941896
Rabbit polyclonal anti-H4K8la	PTM BIO	Cat# PTM-1415RM
Rabbit monoclonal anti-H3	PTM BIO	Cat# PTM-1002
Rabbit polyclonal anti-β-actin	Proteintech	Cat# 20536-1-AP; RRID:AB_10700003
Rabbit polyclonal anti-ALDOA	Proteintech	Cat# 11217-1-AP; RRID:AB_2224626
Rabbit polyclonal anti-PFKP	Proteintech	Cat# 13389-1-AP; RRID:AB_2252278
Rabbit polyclonal anti-GAPDH	Proteintech	Cat# 10494-1-AP; RRID:AB_2263076
Mouse monoclonal anti-Alpha Tubulin	Proteintech	Cat# 66031-1-Ig; RRID:AB_11042766
Rabbit IgG	Proteintech	Cat# B900610
HRP* Goat Anti Rabbit IgG (H+L)	Immunoway	Cat# RS0002
HRP* Goat Anti Mouse IgG (H+L)	Immunoway	Cat# RS0001; RRID:AB_2943495
HRP* Mouse Anti-Rabbit IgG LCS	Abbkine	Cat# A25022; RRID:AB_2893334
Biological samples		
Paired tumor, adjacent non-tumor colorectal tissues from patients with CRC	Department of General Surgery, Xiangya Hospital	N/A
Chemicals, peptides, and recombinant proteins		
DCA	Selleck	Cat# S8615
Rotenone	Selleck	Cat# 2348
Critical commercial assays		
Lactic acid colorimetric assay kit	Jiancheng Bio	Cat# A019-2-1
PFKP activity kit	Solarbio	Cat# BC0535
EpiQuik Total Histone Extraction Kit	Epigentek	Cat# OP-0006-100
BCA quantification kit	Vazyme	Cat# E112-01
Deposited data		
Proteogenomic data of FHC and SW480 cells	This paper	iProx Consortium: IPX0005142001
Experimental models: Cell lines		
FHC	ATCC	N/A
SW480	ATCC	N/A
SW620	ATCC	N/A
HCT116	ATCC	N/A
Software and algorithms		
MaxQuant 1.6.17.0	N/A	https://www.maxquant.org/
Perseus 1.6.15.0	N/A	https://www.maxquant.org/perseus/
clusterProfiler R package	R project	https://www.r-project.org/
MoMo 5.5.0	N/A	https://memesuite.org/meme/tools/momo
Graphpad Prism 6.01	GraphPad Software	https://www.graphpad.com/
ImageJ	N/A	https://imagej.net/
PyMol 2.5	N/A	https://pymol.org/2/

RESOURCE AVAILABILITY

Lead contact

Further information and requests for resources and reagents should be directed to and will be fulfilled by the lead contact, Yongheng Chen (yonghenc@163.com).

Materials availability

This study did not generate any unique new reagent. All reagents used in this study are commercially available.

Data and code availability

Proteogenomic data of FHC and SW480 cells have been deposited at iProx Consortium: IPX0005142001 and are publicly available as of the date of publication.

This paper does not report original code.

Any additional information required to reanalyze the data reported in this paper is available from the lead contact upon request.

EXPERIMENTAL MODEL AND STUDY PARTICIPANT DETAILS

Clinical sample acquisition

The CRC samples used in the study were collected from the Department of General Surgery, Xiangya Hospital. Patients underwent primary curative resection at Xiangya Hospital and received no prior anticancer treatments. The patients were all Han Chinese people. These primary tumor tissues and paired non-cancerous adjacent tissues (>3 cm apart from tumor edge) were surgically resected, collected within 30 min after operation, transferred to sterile freezing vials and snap-frozen in liquid nitrogen. The tissues were stored at −80°C before processed. All patient samples were obtained with the hospital's approval of the Xiangya Hospital Medical Ethics Committee of Central South University in China with written informed consent provided by all participants.

Cell lines and cell culture

Cells (FHC, SW480, SW620 and HCT116) were all purchased from American Type Culture Collection (ATCC, USA). FHC is an intestinal epithelial cell isolated from the large intestine of a 13-week-old embryo. SW480 and SW620 cells are isolated from the large intestine of a 51-year-old male Dukes C colorectal cancer patient. SW480 is from the primary tumor while SW620 is from metastatic cancer, HCT116 cell line was isolated from the colon of an adult male with colon cancer. HCT116 has a mutation in codon 13 of the ras proto-oncogene.

FHC and HCT116 were cultured in RPMI-1640 medium (Gibco, USA) containing 10% fetal bovine serum (NEWZERUM, New Zealand) and 1% penicillin/streptomycin (ECOTOP, China). SW480 and SW620 cells were cultured in Leibovitz's L15 medium (Gibco, USA) containing 10% fetal bovine serum and 1% penicillin/streptomycin. The culture conditions for FHC and HCT116 were 37°C, 5% CO_2, and 95% humidity. The culture conditions for SW480 and SW620 were 37°C, air and 95% humidity. The cells were authenticated using short tandem repeat (STR) method.

METHOD DETAILS

Protein extraction and tryptic digestion

FHC and SW480 cells were washed three times with phosphate buffer saline (PBS) and lysed in lysis buffer (6M Urea, 2M Thiourea, 100 mM ammonium bicarbonate, pH 8.0) supplemented with protease inhibitor cocktail (Targetmol, C0001) followed by 1min of sonication (1s on and 5 s off, amplitude 20%). The lysate was centrifuged at 14000g for 30 min, and the supernatant was collected as whole cell extract. The protein concentration was determined by Bradford assay. The extracted proteins were reduced in 10 mM dithiothreitol (DTT) at 37°C for 60 min and then alkylated in 50 mM iodoacetamide (IAA) at room temperature for 45 min in darkness. The lysate was diluted with 100 mM ammonium bicarbonate and the concentration of urea was reduced to less than 1 M. Samples then went through trypsin (Promega, V5111) digestion (enzyme-to-substrate ratio of 1:50 at 37°C for 18 hours) followed by desalting through SepPak C18 cartridges (Waters, MA) and vacuum-dried by Speed Vac.

Lactylated-peptide enrichment

For lactylated-peptide enrichment, desalted peptides were dissolved in NETN buffer (100 mM NaCl, 1 mM EDTA, 50 mM Tris-HCl, 0.5% NP-40, pH 8.0) and incubated with polyclonal anti-Pan Kla antibody (PTM BIO, PTM-1401) at 4°C overnight on a vertical mixer. Then the protein A/G PLUS-Agarose (SANTA CRUZ, sc-2003) was added after washed with PBS for three times. The incubation went for another 4 hours. Then the agaroses were washed with NETN buffer, ETN buffer (100 mM NaCl, 1 mM EDTA, 50 mM Tris-HCl, pH 8.0) and H_2O for 3 times each. The conjugated peptides were eluted from the agarose with 0.1% trifluoroacetic acid, went through peptide quantification using a Quantitative Colorimetric Peptide Assay (Thermo Fisher, 23275) and vacuum-dried subsequently. Then the samples were desalted with C18 ZipTips (Millipore) according to the manufacturer's instructions.

LC-MS/MS analysis

Peptide samples were analyzed on an Ultimate 3000 LC system (Thermo Fisher Scientific, Waltham, MA) coupled with an LTQ Orbitrap Elite mass spectrometry (Thermo Fisher Scientific, Waltham, MA). Peptides were resuspended in mobile phase A (2% ACN and 0.1% formic acid) and loaded onto an Acclaim™ Pepmap™ 100 C18 preconcentration column (150 μm × 20 mm; Thermo Fisher Scientific) in front of an Acclaim™ Pepmap™ 100 C18 nano column (75 μm × 150 mm; Thermo Fisher Scientific).

Peptides were separated onto the analytical column with a 60 min gradient (buffer A: 0.1 % Formic acid in water; buffer B: 0.1 % Formic acid in 90 % ACN) at a constant flow rate of 300 nL/min (0-50 min, 5 to 45 % of buffer B; 50-55 min, 45% to 80% buffer B; 55-60 min, 80% of buffer B). The eluted peptides were ionized under 2 kV and introduced into mass spectrometry. Mass spectrometry was operated under a data-dependent acquisition mode. For the MS1 full scan, ions with m/z ranging from 350 to 1500 were acquired by Orbitrap mass analyzer at a high resolution of 120,000. The automatic gain control (AGC) was set as 5 × 105. The maximal ion injection time was 50 ms. MS2 acquisition was performed in a top-speed mode and the duty cycle time was 3 s. Precursor ions were selected and fragmented with higher energy collision dissociation (HCD) with normalized collision energy of 32%. Fragment ions were analyzed by ion trap mass analyzer with AGC at 7000. The maximal ion injection time of MS2 was 35 ms and the dynamic exclusion was 60 s.

Peptide identification and protein quantification

Raw files were processed using the MaxQuant computational platform (version 2.1.3.0). Peak lists were searched against Uniprot human database (10/2021). The search engine set cysteine carbamidomethylation as a fixed modification and N-acetylation, oxidation of methionine, lactylation of lysine as variable modifications and mis-cleavages was set to 2. The match-between-runs option was selected. Peptides with a length of at least seven amino-acids were considered and the FDR was set to 1% at the peptide and protein level. Protein identification required at least 2 unique or razor peptides per protein. Relative protein quantification in MaxQuant was performed using the label-free quantification (LFQ) algorithm. Statistical analysis (n = 3) was performed using the R statistical package. Only sample groups with at least 2 valid values were used. Protein contaminants and proteins identified by <2 peptides were excluded from the analysis. MS/MS raw files, as well as results of MaxQuant analysis were deposited to the iProx Consortium with the dataset identifier: IPX0005142001.

Bioinformatic analysis

Wilcoxon rank-sum test was used to identify proteins with significantly different expression between groups. KOG and KEGG analyses were performed using the clusterProfiler R package. Items from KOG, KEGG with p-value < 0.05 were considered significantly enriched. Only lactylated peptides with localization prob $\geq$ 0.75 were used in the subsequent analysis. The peptides were aligned and extended to a width of 15 amino acids using customed R script. The aligned peptides were used to extract motifs using MoMo (motif-x algorithm, https://meme-suite.org/meme/tools/momo); the probability threshold was set to p-value $\leq 10^{-5}$; the default Uniprot Human Proteome dataset (https://www.uniprot.org) was used as the background dataset. Enrichment was determined using default settings (significance level 0.05). Subcellular localization was analyzed using Uniprot database.

Histone extraction

Histones extraction was performed using the EpiQuik Total Histone Extraction Kit according to the manufacturer's instructions (Epigentek, OP-0006-100). Briefly, cells were collected and resuspended in pre-lysis buffer containing protease inhibitor cocktail (Targetmol, C0001). The cells were lysed on ice for 10 min with gentle stirring, followed by centrifugation at 10,000 g for 1 min at 4°C. Then the supernatant was removed and the cell pellet was re-suspended in lysis buffer and incubated on ice for 30 min. Then centrifuged at 12,000 rpm for 5 min at 4°C and balance buffer was added into the supernatant fraction. The histone protein was quantified with Bradford assay and prepared for western blotting.

Western blotting (WB)

Extraction of cell proteins was performed as previously described. The proteins were boiled with SDS-PAGE loading buffer (CWBIO, CW0027) for 5 min. After denaturation, equal amounts of protein in the lysates were separated by SDS-PAGE and then transferred to a polyvinylidene fluoride (PVDF, Millipore) membrane. The membranes were blocked with 5% non-fat milk in phosphate buffer saline containing 0.1% Tween-20 (PBST) for 1 h at room temperature followed by incubation with the indicated primary antibodies at 4°C overnight. After washes with PBST three times, the membranes were incubated with horseradish peroxidase (HRP)-conjugated secondary antibodies. The target proteins were detected using a hypersensitive chemiluminescent (ECL) western HRP substrate and visualized with GeneSys (Syngene, USA).

Immunoprecipitation (IP)

For cell proteins, the cells were lysed in 1 % Triton-X100 (Sigma Aldrich, 9036-19-5) lysis buffer containing protease inhibitor cocktail. The protein was sonicated for 1 min (1s on and 5 s off, amplitude 20%) followed by centrifugation at 12,000 g for 20 min at 4°C. The supernatant was collected and determined by a BCA quantification kit (Vazyme, E112-01). For CRC tissue protein extraction, the tissues were lysed with RIPA (Radio Immunoprecipitation Assay) lysis buffer (Beyotime, P0013B) containing protease inhibitor cocktail. In brief, tissues were washed with saline (0.9% sodium chloride) three times and then were lysed by RIPA buffer. The tissue samples were lysed using a tissue cell-destroyer according to the manufacturer's instructions (NewZongKe, DS1000). Then the tissue protein was sonicated for 1 min (1s on and 5 s off, amplitude

20%) followed by centrifugation at 12,000 g for 20 min at 4°C. The supernatant was collected and determined by BCA quantification assay. The proteins were incubated with corresponding antibodies at 4°C overnight on a vertical mixer. Then the protein A/G PLUS-Agarose (SANTA CRUZ, sc-2003) was added after washed with PBS for three times. The incubation went for another 4 hours. Then the agaroses were washed with 1 % Triton-X100 buffer (cell proteins) or RIPA buffer (tissue proteins) for 5 times. Then the agarose was boiled with SDS-PAGE loading buffer and followed by western blotting.

Two-dimensional gel electrophoresis (2-DE)

Cells (1×10^6) were resuspended in 150 μl rehydration buffer (8 M Urea, 2% CHAPS, 0.5% IPG Buffer, 0.002% bromophenol blue) and three pulses of sonication (10s on and 15s off, amplitude 20%). Cell lysates were centrifugated at 14,000 g and 4°C for 20 min. Centrifuged cell lysates were loaded to isoelectric focusing (IEF) strips (GE Healthcare) for first-dimension electrophoresis with a program comprising: 20 V, 10 h (rehydration); 100 V, 1 h; 500 V, 1 h; 1000 V, 1 h; 2000 V, 1 h; 4000 V, 1 h; 8000 V, 4h. After IEF, strips were incubated in SDS equilibration buffer (50 mM Tris-HCl [pH8.8], 6 M urea, 30% glycerol, 2% SDS, 0.001% bromophenol blue) containing 10 mg/ml DTT) for 15 min and SDS equilibration buffer containing IAA for 15 min. Strips were washed with SDS-PAGE buffer, resolved by SDS-PAGE, and analyzed by immunoblotting.

Intracellular lactic acid determination and PFKP activity assay

The intracellular lactic acid levels were analyzed using a lactic acid colorimetric assay kit (Jiancheng Bio, A019-2-1) according to manufacturer's instructions. The PFKP activity was tested using a PFKP activity kit (Solarbio, BC0535) according to manufacturer's instructions. The data were analyzed in GraphPad Prism 6 with corresponding statistical approaches.

QUANTIFICATION AND STATISTICAL ANALYSIS

Quantification and statistical analysis were conducted in GraphPad Prism 6. Two groups were compared with Prism software (GraphPad 6) using a two-tailed unpaired Student's t-test. The statistical significance is indicated as asterisks (*). A 2-sided P value of < 0.05 was considered statistically significant (*$P < 0.05$, **$P < 0.01$, ***$P < 0.001$).